MODELING THMC CHANGES IN EBS BENTONITE AT HIGH TEMPERATURE

Liange Zheng, Jonny Rutqvist, Jens T. Birkholzer

Lawrence Berkeley National Laboratory (LBNL), Berkeley, California 94720, USA; lzheng@lbl.gov

In geologic repositories for high-level radioactive waste, the transformation of smectite to illite could compromise some beneficiary features of an engineered barrier system (EBS) that is composed primarily of bentonite. It is believed that such illitization could be greatly enhanced at temperatures higher than 100°C and thus could significantly lower the sorption and swelling capacity of bentonite. However, existing experimental and modeling studies on the occurrence of illitization and related performance impacts are not conclusive, in part because the relevant couplings between the thermal, hydrological, chemical, and mechanical (THMC) processes have not been fully represented in the models. Here we present fully coupled THMC simulations of a generic nuclear waste repository in a clay formation with bentonite-backfilled EBS. Two scenarios were simulated for comparison: a case in which the temperature in the bentonite near the waste canister can reach about 200°C and a case in which the temperature in the bentonite near the waste canister peaks at about 100 °C.

The model simulations demonstrate that illitization is in general more significant at higher temperatures. We compared the chemical changes and the resulting swelling stress changes for two types of bentonite: Kunigel-VI and FEBEX bentonite. For Kunigel-VI bentonite, the decrease in smectite volume fraction is about 0.035–0.038 (which is equal to about 11–12% of the initial volume fraction of smectite) for the 200°C base case scenario. For FEBEX bentonite, the decrease in smectite volume fraction is 0.01–0.018 (or 1.6–3% of the initial amount). Chemical changes lead to a reduction in swelling stress, which is more pronounced for Kunigel-VI bentonite than for FEBEX bentonite. For Kunigel-VI bentonite, a reduction in swelling stress is up to 16–18% for the 200°C base case scenario, whereas for FEBEX bentonite, the model shows only about 1.5–3% reduction in swelling stress.

I. INTRODUCTION

Radioactive waste from spent fuel emanates a significant amount of thermal energy, due to decay processes, which causes temperature increases in the surrounding environment of geologic repository tunnels, particularly in the early stages of waste emplacement. The temperature to which the EBS and natural rock can be exposed is one of the most important design variables for a geological repository, because it determines waste package spacing, distance between disposal galleries, and therefore the overall size (and cost) of a repository for a given amount of heat-emanating waste.[1] This is especially important for a clay repository, because argillaceous rocks have relatively small heat conductivity. A thermal limit of about 100°C is currently imposed in all disposal concepts throughout the world that involve the use of bentonite buffer and backfill materials, despite differences in design concepts.[2] Chemical alteration and the subsequent changes in mechanical properties are among the determining factors. A high temperature could result in chemical alteration of buffer and backfill materials (bentonite) within the EBS through illitization and cementation, which compromise the function of these EBS components by reducing their plasticity and capability to swell when wetting.[3,4,5] The swelling capability of clay minerals within the bentonite is important for sealing gaps between bentonite blocks, between bentonite and other EBS components, and between the EBS and the surrounding host rock, and also provides confining pressure on the surrounding rock damage zone near emplacement tunnels, which helps the sealing of fractures.

Regarding the concern of chemical alteration and the associated mechanical changes, Wersin et al.[5] concluded after reviewing a number of data sets that the criterion of 100°C for the maximum temperature within the bentonite buffer is overly conservative. Their conclusion was based on findings that no significant changes in bentonite hydraulic properties occur at temperatures of at least 120°C under wet conditions and that bentonite is chemically stable to much higher temperatures under dry conditions. However, the impact of higher temperature on bentonite behavior and the consequences on repository performance, remain largely open questions. While various studies shed light on certain aspects of this question, there is a lack of studies that integrate the relevant THMC processes and consider the interaction between the EBS and the host rock.

In this paper, we use coupled THMC modeling to evaluate the chemical alteration and mechanical changes in EBS bentonite surrounded by a clay formation, to

provide necessary information for decisions on temperature limits and to motivate more studies on this issue. Two temperature scenarios were simulated for comparison: a case in which the temperature in the bentonite near the waste canister can reach about 200°C, and a case in which the temperature in the bentonite near the waste canister peaks at about 100°C. In each scenario, two types of EBS bentonite were evaluated: Kunigel-V1 bentonite[6] and FEBEX bentonite.[7] The host rock properties were representative of Opalinus Clay. [8,9]

II. THE THMC SIMULATOR — TOUGHREACT-FLAC

Numerical simulations are conducted with TOUGHREACT-FLAC, which sequentially couples the multiphase fluid flow and reactive transport simulator, TOUGHREACT,[10] with the geomechanical code FLAC3D.[11] The coupling of TOUGHREACT and FLAC was initially developed in Zheng et al.[12] to provide the necessary numerical framework for modeling fully coupled THMC processes. The coupled simulator was equipped with a linear elastic swelling model[12,13] to account for swelling as a result of changes in saturation and pore-water composition and the abundance of swelling clay.[14]

III. MODEL DEVELOPMENT

III.A. Modeling Scenario

The 2-D cross-sectional model is applied to a hypothetical bentonite-backfilled nuclear waste repository in a clay formation. The repository example involves a horizontal nuclear waste emplacement tunnel at 500 m depth (Fig.1). [13] The Z-axis is set as vertical in the model, while the horizontal Y- and X-axes are aligned parallel and perpendicular to the emplacement tunnel, respectively (Fig.1). An initial stress field is subjected to the self-weight of the rock mass. Zero normal displacements are prescribed on the lateral boundaries of the model. Vertical displacements are prevented at the bottom. The model simulation was conducted in a nonisothermal mode with a time-dependent heat power input, [13] adopted from the heat load developed within the U.S. DOE's Used Fuel Disposition campaign as a generic disposal system environment for Pressurized Water Reactor (PWR) used nuclear fuel. This heat load is then scaled in the 2D model to represent a certain line load, which depends on the assumed spacing between individual waste packages along an emplacement tunnel. Initially, the EBS bentonite has a water saturation of 65% (which was used in other models[13] and it similar to the initial water saturation of FEBEX bentonite[7]) and the clay formation is fully saturated. From time zero, the EBS bentonite simultaneously undergoes resaturation, heating, chemical alteration, and stress changes.

Thermal and hydrological parameters for bentonite and clay rocks are listed in Table I. The majority of the parameters for the EBS bentonite are based on the properties of Kunigel-VI bentonite,[15] and those for the clay formation are from Thury.[16] Permeability for the clay formation is from Soler,[17] and that for the bentonite is from Japan Nuclear Cycle Development Institute (JNC).[18]

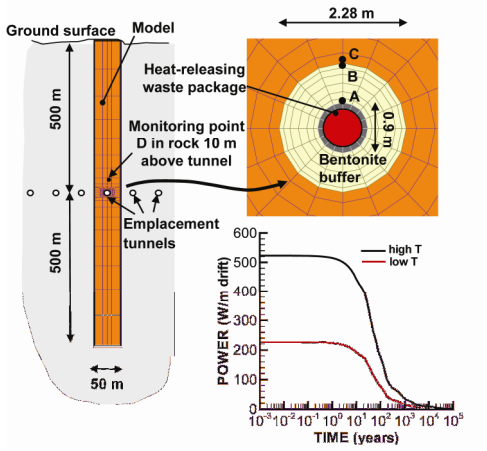

Fig. 1. Domain for the test example of a bentonite back-filled horizontal emplacement drift at 500 m.[13] Point A is inside the bentonite near the canister, point B is inside the bentonite and near the bentonite-clay formation interface, point C is inside the clay formation and near the interface.

TABLE I. Thermal and hydrological parameters.

Parameter	Clay Formation	EBS Bentonite
Grain density [kg/m^3]	2700	2700
Porosity ϕ	0.162	0.33
Saturated permeability [m^2]	2.0×10^{-20}	2.0×10^{-21}
Relative permeability, k_{rl}	m = 0.6, S_{rl} = 0.01	$K_{rl} = S^3$
Van Genuchten α [1/Pa]	6.8×10^{-7}	3.3×10^{-8}
Van Genuchten m	0.6	0.3
Compressibility, β [1/Pa]	3.2×10^{-9}	5.0×10^{-8}
Thermal expansion coeff., [1/^{o}C]	1.0×10^{-5}	1.5×10^{-4}
Dry specific heat, [J/kg ^{o}C]	860	800
Thermal conductivity [W/m ^{o}C] dry/wet, Λ_d/Λ_w	1.47*/1.7$^\$$	1.1/1.5
Tortuosity for vapor phase	$\phi^{1/3} S_g^{10/3}$	$\phi^{1/3} S_g^{10/3}$
Bulk modulus, (GPa)	4.17	0.02
Shear modulus, (GPa)	1.92	0.0067

*calculated by $\Lambda_d=(1-\phi)\Lambda_w$

$^\$$from http://www.mont-terri.ch/internet/mont-terri/en/home/geology/key_characteristics.html

The two bentonites selected in this study, FEBEX and Kunigel-VI, differ in their mineralogy and initial pore-water composition. They also have distinct hydrological and thermal parameters; however, the most relevant of these, thermal conductivity and permeability, are actually fairly similar for both bentonites. The thermal conductivity for saturated Kunigel-VI bentonite is 1.5W/m°C, compared to 1.3 W/m°C for FEBEX bentonite,[7] and the permeability for Kunigel-VI bentonite is about 2×10^{-21} m^2 compared to a range of 3.75×10^{-21} to 1×10^{-21} m^2 reported for FEBEX bentonite.[7,19,20] Therefore, in this paper, we use identical thermal and hydrological parameters for both bentonites, but different chemical parameters. By having the same thermal and hydrological parameters, we can isolate the effect of variation in chemical parameters on stress changes.

III.B. Mechanical Model

To consider the swelling due to both moisture and chemical changes, we include the stress due to changes in chemical concentration and abundance of swelling clay:

$$d\sigma_s = 3K\beta_{sw}dS_l - A_n dC + A_{sc}dm_s \quad (1)$$

where K is the bulk modulus, β_{sw} is a moisture swelling coefficient and S_l is liquid saturation. In this paper, β_{sw} is set to 0.048 for Kunigel-VI bentonite, which was calibrated to the swelling pressure of 1 MPa (Ref. 21) under the condition that bentonite is saturated with a dilute solution (e.g., deionized water). β_{sw} is 0.238 for FEBEX bentonite.[18] The bulk modulus K is 20 MPa for both bentonites.[22] A_n is a constant that linearly relates chemical concentration (C) variation and the corresponding stress change. A_n is typically calculated from swelling pressures measured using different solutions (e.g., deionized water versus 1 M NaCl solution) that are used to saturate the bentonite. Laredj et al.[23] proposed the following expression for A_n:

$$A_n = \frac{(5.312\ln C - 23.596)}{\sqrt{C}} - \frac{7.252\times10^{-4}}{C^2} \quad (2)$$

A_{sc} is a constant that relates the change in mass fraction of swelling clay, m_s, to change in stress. An empirical value is derived from measured swelling pressure for bentonite materials of different smectite mass fraction,[14] which is 2.5×10^6 Pa^{-1} for Kunigel-VI bentonite and 6.5×10^6 Pa^{-1} for FEBEX bentonite. The linear elastic model provides a fairly accurate calculation of the swelling pressure after bentonite become fully saturation and is not reliable to catch the transient swelling behavior during saturation, which is acceptable for the long term simulation presented in the paper. Swelling models[30] that consider the interaction between micro- and macro-structure is needed to describe the transient swelling behavior.

III.C. Chemical Model

TABLE II. Mineral volume fraction (dimensionless, ratio of mineral volume to total volume of medium) of the Kunigel-VI,[6] FEBEX bentonite[7,26,27] and Opalinus Clay.[8,9]

Mineral	EBS Bentonite: Kunigel-V1	EBS Bentonite: FEBEX	Clay formation: Opalinus Clay
Calcite	0.016	0.0065	0.093
Dolomite	0.018	0.0	0.050
Illite	0.000	0.0	0.273
Kaolinite	0.000	0.0	0.186
Smectite	0.314	0.6	0.035
Chlorite	0.000	0.0	0.076
Quartz	0.228	0.026	0.111
K-Feldspar	0.029	0.0065	0.015
Siderite	0.000	0.0	0.020
Ankerite	0.000	0.0	0.045

TABLE III. Pore-water composition of Kunigel-VI bentonite, [15] FEBEX bentonite [24] and Opalinus Clay.[25]

	EBS Bentonite: Kunigel-V1	EBS Bentonite: FEBEX	Clay formation: Opalinus Clay
pH	8.40	7.72	7.40
Cl	1.50E-05	1.60E-01	3.32E-01
SO_4^{-2}	1.10E-04	3.20E-02	1.86E-02
HCO_3^-	3.49E-03	4.1E-04	5.18E-03
Ca^{+2}	1.37E-04	2.2E-02	2.26E-02
Mg^{+2}	1.77E-05	2.3E-02	2.09E-02
Na^+	3.60E-03	1.3E-01	2.76E-01
K^+	6.14E-05	1.7E-03	2.16E-03
Fe^{+2}	2.06E-08	2.06E-08	3.46E-06
SiO_2(aq)	3.38E-04	1.1E-04	1.10E-04
AlO_2^-	1.91E-09	1.91E-09	3.89E-08

In these generic cases, it is assumed that the host-rock properties are representative of Opalinus Clay, 8,9 that the EBS backfill is composed of either Kunigel-VI bentonite6 or FEBEX bentonite.7 The mineral compositions of the bentonites and the clay formation are listed in Table II. The pore-water composition of the Kunigel-VI bentonite15, FEBEX bentonite24 and the clay formation25 are given in Table III. Illitization is modeled as the dissolution of smectite and precipitation of illite. The overall reaction can be written as:

$$\text{Smectite} + 0.52H^+ + 0.63AlO_2^- + 0.6K = \text{illite} + 0.26H_2O + 0.08Mg^{+2} + 0.33Na^+ + \quad (3)$$

$0.5SiO_2(aq)$

IV. MODEL RESULTS

We present model results for two temperature regimes and two cases of bentonite, focusing on the temporal evolution of smectite volume fraction and swelling stress. A complete set of THMC evolutions and the sensitivity analysis of key chemical and mechanical parameters are given in Liu et al.[14] and Zheng et al.[28]

IV.A. Case for Kunigel-VI Bentonite

Although clay formation is an indispensible part of the model as described above, we focus on the EBS bentonite in this paper because the thermal limit is more critical near the waste packages. The temporal evolution at two monitoring points (see Fig. 1 for their positions) is used to present thermal, hydrological, chemical, and mechanical results: point A is inside the bentonite near the canister, point B is inside the bentonite near the bentonite/clay formation interface. The heat release rates have been set to generate two cases for comparison: a "high T" case and a "low T" case. Temperature evolutions at point A are given in Fig. 2, comparing the two cases. Pore pressure increases as a result of resaturation and heating. The "high T" case exhibit much higher pore pressure than the "low T," with a difference of about 5 MPa after 1,000 years (Fig. 3). It takes about 20 years for the low T case to fully saturate the bentonite backfill, compared to about 30 years for the "high T" case. Note that the temperature and pore pressure evolution are the same for Kunigel-VI and FEBEX bentonite are the same as the same TH parameter are assumed.

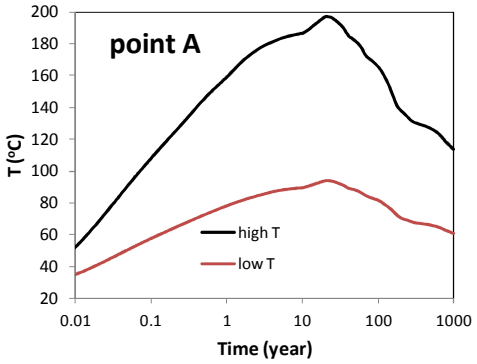

Fig. 2. Temperature evolution at point A.

Model results show that illitization occurs in the EBS bentonite, as shown by the smectite and illite volume fraction changes at points A and B in Figs. 4 and 5. In addition to temperature effects, illitization is affected by the initial disequilibrium between the pore-water solution and the mineral phase. Initially, the pore water in the bentonite buffer is oversaturated with respect to illite and undersaturated with respect to smectite. Also, the pore water in the clay formation contains a much higher concentration of K and Al, and thus provides a source of Al and K for the EBS bentonite alteration through diffusion and advection. Note that the increase in Al and K concentrations in bentonite is caused not only by diffusion and advection, but also by the dissolution of other minerals, such as K-feldspar. The pore water in the clay formation furthermore has a higher concentration of Mg and Na, which inhibits illitization. But it seems that the factors promoting illitization outpace those against illitization. At the end of 1,000 years, the smectite volume fraction in the bentonite decreases by 0.035 (or 11%) for the "high T" case and 0.006 (or 2%) for the "low T" case at point A, which corresponds to an illite volume fraction increase of similar magnitude. Clearly, the "high T" case demonstrates stronger illitization than the "low T" case. The smectite volume fraction decrease by about 0.038 at point B, slightly more than at point A.

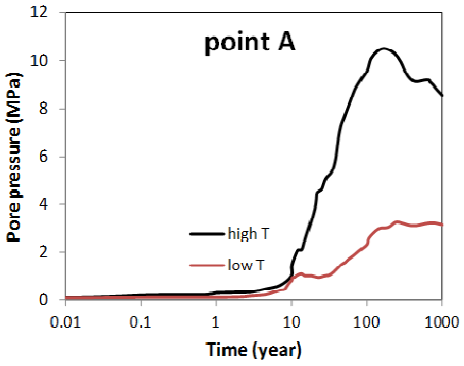

Fig. 3. Pore pressure evolution at point A.

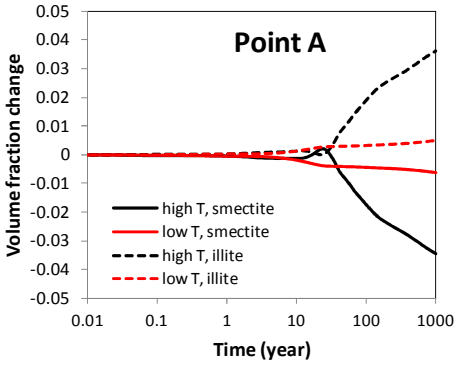

Fig. 4. Evolution of volume fraction change at point A for Kunigel-VI bentonite. Volume fraction change shown in the Y-axis is equal to the volume fraction of smectite/illite at a given time minus the initial volume fraction (see Table II), so a negative value means dissolution and a positive value means precipitation.

Fig. 6 shows the stress changes at point B for both "low T" and "high T" cases (results at point A are similar

to those at point B and therefore not shown in the paper). Several processes combine to drive the stress in bentonite up to around 5.1 MPa for the "low T" and 11.5 MPa for the "high T" case after 1,000 years, including the increase in pore pressure due to hydration and thermal pressurization (a processes caused by the difference in thermal expansion of the fluid and solid host rock), bentonite swelling, and thermal expansion. In comparison with the "low T" case, clearly the stronger thermal pressurization in the "high T" case leads to much higher stress in the bentonite. For both the "high T" and "low T" case, the total stress within the buffer has the major contribution from pore pressure increases, with minor contributions from swelling and thermal stress. Increase in pore pressure in general lowers the mechanical stability of bentonite whereas increase in swelling and thermal stress improves the stability. Because mechanical failure (formation of micro-fractures) is not included in the current model, further study is needed to evaluate the overall mechanical consequence of increase in stress due to heating.

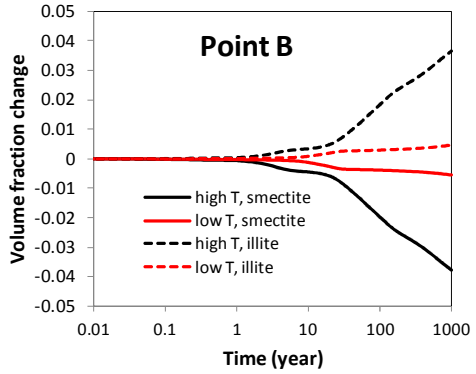

Fig. 5. Evolution of volume fraction change of smectite and illite at point B for Kunigel-VI bentonite.

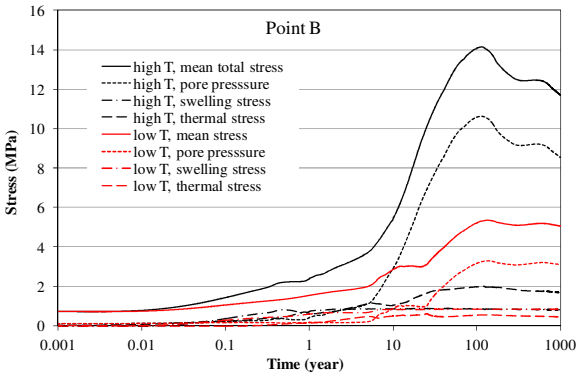

Fig. 6. Evolution of mean total stress, pore pressure, and thermal stress at point B for Kunigel-VI bentonite for the "low T" and "high T" scenario, respectively.

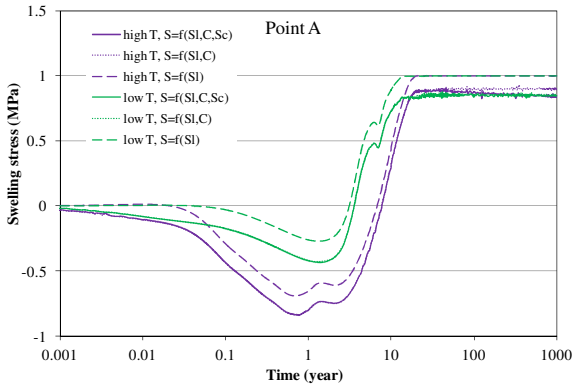

Fig. 7. Simulation results of swelling stress at point A for Kunigel-VI bentonite for the "low T" and "high T" scenarios, respectively.

The constitutive relationship described by Equation (1) provides an opportunity to further evaluate the effects of different types of chemical changes on the swelling stress and compare these to the swelling induced by saturation changes. In order to isolate the contributions of ion concentration changes versus smectite changes to swelling stress changes, we present three sets of calculated swelling stress. In the first set, denoted in Figs. 7 and 8 as "S=f(Sl,C,Sc)", the swelling stress is calculated according to Equation (1) as a function of liquid saturation changes (Sl), ion concentration (C) changes, and smectite (Sc) changes. In the second set, denoted as "S=f(Sl,C)", the contribution from smectite changes in Equation (1) is disregarded, and the swelling stress is only a function of liquid saturation and ion concentration. In the third set, denoted as "S=f(Sl)", all chemical effects are neglected, and the swelling stress is only a function of liquid saturation changes.

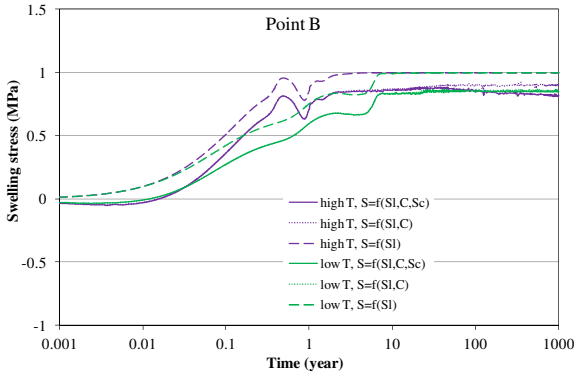

Fig. 8. Simulation results of swelling stress at point B for Kunigel-VI bentonite for the "low T" and "high T" scenarios, respectively.

At early times (< 20 years), results for "S=f(Sl,C,Sc)" and "S=f(Sl,C)" are indistinguishable (Figs. 7 and 8),

indicating that smectite changes have not yet contributed to stress increases. We recall that the volume fraction of smectite shows significant changes only after about 20 years (see Fig. 5). Ion concentration changes start to affect stress at early times (< 20 years) and maintain such effects afterwards. Initially, the bentonite near the canister undergoes desaturation and therefore a negative swelling stress is observed for a few years (see Fig. 7 for changes at point A). For the "low T" case, the ion concentration increase leads to a drop in swelling stress of about 0.14 MPa at the end of the 1,000-year simulation period, and the dissolution of smectite reduces the swelling stress a little further, by about 0.003 MPa. For the "high T" case, after 1,000 years, ion concentration changes cause about a 0.1 MPa decrease in swelling stress, and the loss of smectite due to dissolution results in about a 0.05 MPa reduction in swelling stress. In general, the chemical changes in bentonite have a fairly moderate effect on swelling stress, about 14% swelling stress reduction due to chemical change for the "low T" case and about 15% swelling stress reduction for the "high T" case at point A (Fig. 7). The stress changes near the EBS-clay formation (point B) interface behave similarly to those near the canister, except that the stress starts to increase earlier due to faster resaturation. In terms of the total stress, the decrease in swelling stress accounts for about a 1.4–1.7% reduction in the total stress.

IV.B. Case for FEBEX Bentonite

In this section, we present model results using FEBEX bentonite as the EBS. Compared to Kunigel-VI bentonite[6], the FEBEX bentonite[7] has higher fraction of smectite and a higher swelling capacity. Specifically, the FEBEX bentonite differs from Kunigel-VI in the following aspects:

1. In terms of aqueous chemistry, FEBEX bentonite has a higher ion concentration in pore water, as shown in Table III. The concentration of major cations, i.e., Ca, Mg, Na, K is about two orders of magnitude higher than for Kunigel-VI bentonite, which could affect the illitization over the course of heating and hydration.
2. In terms of mineralogical composition, the most pronounced difference between FEBEX and Kunigel-VI bentonite is the content of smectite, with FEBEX bentonite containing about 60 vol% smectite and Kunigel-VI bentonite about 31 vol% smectite (see Table II). FEBEX bentonite has also less K-feldspar, which could affect illitization.
3. FEBEX bentonite also has a higher swelling pressure, ranging from 4.5 MPa (Ref. 29) to 7 MPa (Ref. 7), compared to Kunigel-VI bentonite, which has swelling pressure of around 1 Mpa (Ref. 21) measured using distilled water.

Figs. 9 compares the smectite volume fraction changes for the two bentonites at point B (changes at point A is similar to those at point B). In the "high T" scenario, there is clearly less smectite dissolution (and corresponding illite precipitation) in the FEBEX bentonite. The smectite volume fraction decreases by about 0.01 at point A and by 0.018 at point B, compared to about 1.6% and 3% of the initial smectite volume fraction, respectively. This is significantly less than the decrease of 0.035 to 0.038 (11–12% of the initial amount) for Kunigel-VI bentonite. In the "low T" scenario, the amount of smectite dissolution is similar for both bentonites. The differences in dissolved smectite between "high T" and "low T" scenarios for FEBEX bentonite are smaller than that for Kunigel-VI bentonite.

Because FEBEX bentonite has higher swelling pressure, the total stress for FEBEX bentonite at points A and B is 3–4 MPa higher than for Kunigel bentonite after 1,000 years.

Compared to Kunigel-VI bentonite, the swelling stress evolution for FEBEX bentonite (Fig. 10) shows two distinct features. First, the change in ion concentration has a minimal effect on the swelling stress, because the ion concentration of the pore water in FEBEX bentonite is fairly close to that of the clay formation. As a result, the ion concentration in pore water for FEBEX bentonite increases only moderately, which changes the swelling stress insignificantly. In comparison, about 0.1 MPa swelling stress reduction due to ion concentration has been observed for Kunigel bentonite. Second, the FEBEX bentonite exhibits more stress reduction due to smectite dissolution. Despite the fact that less smectite dissolution has been observed for FEBEX bentonite (Fig. 9), the higher A_{sc} (a parameter that relates swelling stress to the abundance of smectite) for FEBEX bentonite leads to a slightly higher reduction in swelling stress.

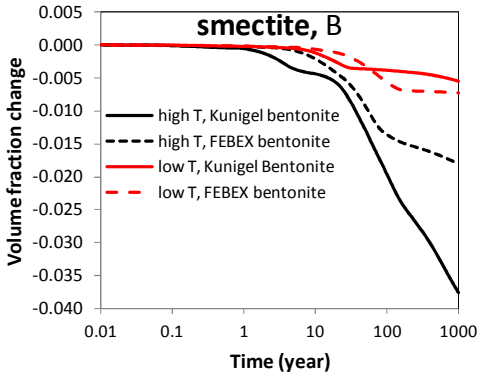

Fig. 9. Evolution of smectite volume fraction at point B for Kunigel-VI and FEBEX bentonite.

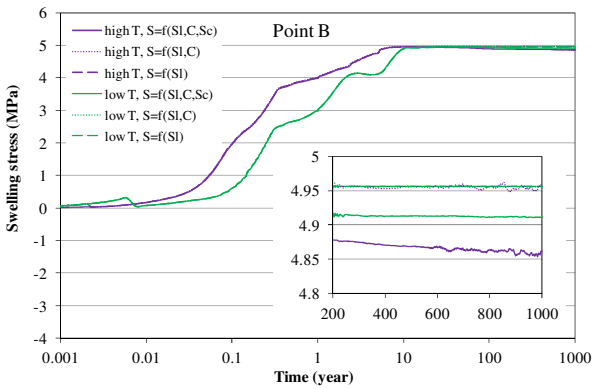

Fig. 10. Simulation results of swelling stress at point B for the "low T" and "high T" scenarios, for FEBEX bentonite.

Table IV lists the stress reduction by ion concentration and smectite dissolution at point A for Kunigel-VI and FEBEX bentonite. In total, chemical changes lead to about a 0.15 MPa stress change for Kunigel-VI bentonite and 0.08 MPa for FEBEX bentonite. Relative to the swelling stress obtained due to "S=f(Sl)", chemical change causes about a 15% reduction in swelling stress for Kunigel-VI bentonite, but only 1.6% for FEBEX bentonite. Model results at point B lead to similar observations in terms of the difference between Kunigel-VI and FEBEX bentonite, although the specific values differ slightly from those at point A.

Table IV. Geochemically induced swelling stress for Kunigel and FEBEX bentonite at point A for "high T" scenario.

Kunigel	Stress reduction by ion concentration, MPa	0.1
	Stress reduction by ion concentration, (%)	10%
	Stress reduction by smectite dissolution Mpa	0.05
	Stress reduction by smectite dissolution (%)	5%
FEBEX	Stress reduction by ion concentration, Mpa	0.006
	Stress reduction by ion concentration, (%)	0.1%
	Stress reduction by smectite dissolution, Mpa	0.076
	Stress reduction by smectite dissolution (%)	1.5%

V. CONCLUSIONS

This study investigates the impact of strongly elevated temperature on the bentonite backfill in a geologic repository for radioactive waste. We use coupled THMC modeling to evaluate the chemical alteration and associated mechanical changes in a generic repository and consider the interaction between EBS bentonite and the clay formation. Two main scenarios were developed for comparison: a "high T" case in which the temperature near the waste package reaches about 200°C, and a "low T" scenario in which the temperature peaks at about 100°C.

Our model results indicate the occurrence of some degree of illitization in the EBS bentonite. In general, illitization in the bentonite is enhanced at higher temperature. Because of their different chemical properties, two types of bentonite (Kunigel-VI and FEBEX bentonite) exhibit differences in terms of the degree of illitization. For Kunigel-VI bentonite, the decrease in the smectite volume fraction is about 0.035–0.038 (about 11–12% of the initial volume fraction of smectite) for the 200°C base case scenario. For FEBEX bentonite, the decrease in smectite volume fraction is 0.01–0.018 (1.6–3% of the initial amount). Chemical changes lead to a reduction in swelling stress, which is more pronounced for Kunigel-VI bentonite than for FEBEX bentonite. For Kunigel-VI bentonite, the simulated reduction in swelling stress is up to 16–18% for the 200°C base case scenario, whereas for FEBEX bentonite, the model shows only about 1.5–3% reduction in swelling stress. The reasons are that (1) FEBEX bentonite exhibits a lesser degree of illitization and (2) FEBEX bentonite has a higher swelling capacity so that the relative reduction in swelling stress is fairly small.

The major limitations of current model are the negligence of chemical interaction between bentonite and canister and possible generation of gas phase and the lack of appropriate HM coupling, which warrant further refinement of the THMC models. Despite of these limitations, the modeling work in the paper leads to the tentative conclusion that an argillite repository with bentonite EBS could sustain temperatures higher than 100°C as far as illitization concerns, with the following reasons:

1. Despite illitization in the bentonite backfill and the surrounding clay formation is enhanced at higher temperature, such enhancement is fairly limited even at 200°C due to other constrains on illitization such as the limited supply of K and Al.
2. The effect of illitization on swelling pressure is rather moderate, in particular for the FEBEX bentonite which has a high initial swelling capacity; thus the functionality of EBS is not necessarily compromised, and using a bentonite with high swelling capacity could diminish undesirable consequences (if any) of illitization.

However, elevated temperature results in higher stress, especially higher pore pressure which might reduce the mechanical stability of bentonite. Further modeling and experimental studies are required.

ACKNOWLEDGMENTS

This work was funded by the U.S. Department of Energy, Used Fuel Disposition Program.

REFERENCES

1. S.T. HORSEMAN and T. J. MCEWEN, *Engineering Geology* 41, 5-16, (1996)
2. T.W. HICKS, M.J. WHITE, and P.J. HOOKER, "Role of Bentonite in Determination of Thermal Limits on Geological Disposal Facility Design", Report 0883-1, Version 2, Falson Sciences Ltd., Rutland, UK, (2009).
3. R. PUSCH and O. KARNLAND, *Engineering Geology* 41: 73-85, (1996).
4. R. PUSCH, J. KASBOHM and H. T. M. THAO, *Applied Clay Science* 47(1–2): 113-119, (2010)
5. P. WERSIN, L.H. JOHNSON, and I.G. MCKINLEY, *Physics and Chemistry of the Earth* 32: 780-788, (2007).
6. M. OCHS, b. LOTHENBACH, M. SHIBATA, and M. YUI, *Physics and Chemistry of the Earth*, Parts A/B/C 29(1): 129-136, (2004).
7. ENRESA, "Full-scale engineered barriers experiment for a deep geological repository in crystalline host rock FEBEX Project", European Commission, EUR 19147 EN, (2000).
8. P. BOSSART, "Characteristics of the Opalinus Clay at Mont Terri," http://www.montterri.ch/internet/montterri/en/home/geology/key_characteristics.parsys.49924.DownloadFile.tmp/characteristicsofopa.pdf, (2012).
9. M. LAUBER, B. BAEYENS and M. H. BRADBURY, "Physico-Chemical Characterisation and Sorption Measurements of Cs, Sr, Ni, Eu, Th, Sn and Se on Opalinus Clay from Mont Terri". PSI Bericht Nr. 00-10 December 2000 ISSN 1019-0643, (2000).
10. T. XU, N. SPYCHER, E. SONNENTHAL, G. ZHANG, L. ZHENG, and K. PRUESS, *Computers & Geosciences*, 37(6), 763-774, 2011.
11. ITASCA, "FLAC3D V4.0, Fast Lagrangian Analysis of Continua in 3 Dimensions, User's Guide" Itasca Consulting Group, Minneapolis, Minnesota, (2009).
12. L. ZHENG, et al, "Modeling Radionuclide Transport in Clays". Lawrence Berkeley National Laboratory, FCRD-URD-2012-000128, (2012).
13. J. RUTQVIST, et al., *Rock Mechanics and Rock Engineering*, 1-20, (2013).
14. H.H. Liu, et al., "Report on THMC modeling of the near field evolution of a generic clay repository: Model validation and demonstration", (FCRD-UFD-2013-000244), U.S. DOE Used Fuel Disposition Campaign, (2013).
15. E. SONNENTHAL, Chapter 5 in: "Birkholzer, J. Rutqvist, E. Sonnenthal, and D. Barr, Long-Term Permeability/Porosity Changes in the EDZ and Near Field due to THM and THC Processes in Volcanic and Crystalline-Bentonite Systems, DECOVALEX-THMC Project Task D Final Report", (2008).
16. M. THURY, *Rendus Physique* 3(7-8), 923-933, (2002).
17. J.M., SOLER, *Journal of Contaminant Hydrology* 53(1–2), 63-84, (2001).
18. JNC, "H12, Project to Establish the Scientific and Technical Basis for HLW Disposal in Japan. Second Progress Report on Research and Development for the Geological Disposal of HLW in Japan. Supporting Report 2, Repository Design and Engineering Technology" JNC TN1410 2000-003, (2000).
19. Y. CHEN, et al., *Computers and Geotechnics* 36(8): 1308-1329, (2009).
20. L. ZHENG, et al., *Journal of Contaminant Hydrology*, 126(1–2): 45-60, (2011).
21. L. BÖRGESSON, et al., *Int. J. Rock Mech. & Min. Sci.* 38, 105-127, (2001).
22. J. Rutqvist, *Computers & Geosciences*, 37, 739–750, (2011).
23. N. Laredj, et al., *Journal of Porous Media* 13(8): 743-748, (2010).
24. A. Fernández, et al., Pore water chemistry of the FEBEX bentonite. *Mat. Res. Soc. Symp. Proc.* 663, 573–588, (2001).
25. A. Fernández, et al., *Physics and Chemistry of the Earth, Parts A/B/C* 32(1-7): 181-195, (2007).
26. A. FERNÁNDEZ, et al., *Physics and Chemistry of the Earth, Parts A/B/C* 29(1): 105-118, (2004).
27. S. RAMÍREZ, et al., *Applied Clay Science* 21(5–6): 257-269, (2002)
28. L. ZHENG, et al., "Investigation of Coupled Processes and Impact of High Temperature Limits in Argillite Rock", FCRD-UFD-2014-000493, (2014).
29. E. CASTELLANOS, et al., *Physics and Chemistry of the Earth*, Parts A/B/C 33, Supplement 1(0): S516-S526, (2008).
30. A. GENS, Géotechnique 60, 3-74, (2010)